Journal of Cell Science 105, 1025-1043 (1993)
Printed in Great Britain © The Company of Biologists Limited 1993

Ezrin is concentrated in the apical microvilli of a wide variety of epithelial cells whereas moesin is found primarily in endothelial cells

Mark Berryman, Zsofia Franck and Anthony Bretscher*

Section of Biochemistry, Molecular and Cell Biology, Biotechnology Building, Cornell University, Ithaca, NY 14853, USA

*Author for correspondence

SUMMARY

Ezrin and moesin are two cytoskeletal proteins originally purified from human placenta that are 74% identical in overall protein sequence. They are believed to be membrane-cytoskeletal linking proteins because they share sequence homology with erythrocyte band 4.1 and colocalize with actin specifically in microvilli and membrane ruffles in cultured cells. To determine if ezrin and moesin share similar distributions in vivo, we studied their localizations with respect to F-actin in tissue sections. Surprisingly, ezrin and moesin exhibited very different cellular distributions. Ezrin was highly concentrated and colocalized with actin on the apical surface of many epithelial cell types. During enterocyte differentiation, the pattern of expression and redistribution of ezrin was consistent with it performing a role in microvillus assembly. Immunoelectron microscopy in differentiated cells revealed that ezrin was restricted mainly to the plasma membrane of microvilli and other actin-rich surface projections. Moesin was found in endothelial cells and was also enriched in the apical microvilli of a restricted set of epithelial cells. All polarized cell types with abundant microvilli contained one or both proteins, suggesting that ezrin and moesin perform related functions. However, the differential expression of ezrin and moesin indicates that they have distinct properties, which are uniquely adapted to specific cell types.

Key words: actin, ezrin, moesin, microvilli, epithelial polarity, endothelial cells

INTRODUCTION

The organization of the actin cytoskeleton is determined by a host of functionally diverse microfilament-associated proteins. The specific expression and regulation of these proteins contributes to the cellular morphology, motility, and other specialized functions of cells. How does a cell assemble specific actin-containing structures? To address this question, our past efforts have focused on the characterization of the intestinal microvillus cytoskeleton, since its components may include proteins that are important for the assembly and stability of microvilli. The isolated intestinal microvillus cytoskeleton contains, in addition to actin, three major proteins, villin, fimbrin and brush border myosin I, and some minor proteins, one of which is ezrin (Bretscher, 1991; Louvard et al., 1992). Among the three major proteins, villin is the first to accumulate at the apical surface of enterocytes during intestinal development and during cellular differentiation in the adult; fimbrin and myosin I appear at later stages of microvillus assembly and probably help to modify pre-existing microvilli (Ezzel et al., 1989; Heintzelman and Mooseker, 1990a,b; Maunoury et al., 1988; Shibayama et al., 1987). The introduction of villin into cells that normally do not contain this protein, by either transient cDNA expression or direct protein microinjection, leads to a modification of the cell surface to yield abundant large microvilli (Franck et al., 1990; Friederich et al., 1989, 1992). Although the results of these studies are consistent with a role for villin in microvillus assembly, this protein is only expressed in a small subset of cell types that display these structures (Bretscher et al., 1981; Drenckhahn and Mannherz, 1983; Ezzel et al., 1989; Maunoury et al., 1988; Robine et al., 1985). Therefore, villin may be required for the proper assembly of certain types of microvilli but does not appear to be utilized for the formation of all types of microvilli.

Although the specific mechanisms that drive microvillus assembly may vary among different cell types, one might expect to uncover one or more proteins that are common to all mechanisms. Could ezrin participate in assembly? Ezrin is an authentic component of the microvillus cytoskeleton of intestinal epithelial cells (Bretscher, 1983) and gastric parietal cells (Hanzel et al., 1989, 1991; Urushidani et al., 1989). In addition, ezrin is concentrated in microvilli and other actin-rich surface structures in a wide variety of cultured cell lines (Birgbauer and Solomon, 1989; Bretscher, 1983, 1989; Goslin et al., 1989; Gould et al., 1986; Pakkanen et al., 1987, 1988; Pakkanen, 1988). We initially wished to determine the extent to which ezrin is distributed and specifically localized to microvilli in vivo. However, this analysis is potentially complicated by the recent discovery that ezrin is one member of a family of

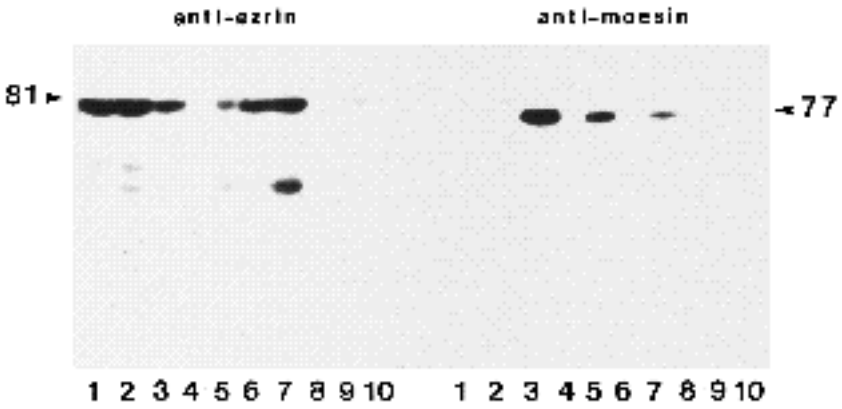

Fig. 1. Detection of ezrin and moesin in various mouse tissues. Tissues were homogenized in Laemmli sample buffer, boiled, and clarified by centrifugation. Protein extracts were run on SDS-PAGE and blotted with antibody specific for ezrin or moesin; ~25 mg of protein was loaded in each lane. Lanes 1, small intestine; lanes 2, epithelial cells isolated from small intestine; lanes 3, lung; lanes 4, liver; lanes 5, spleen; lanes 6, stomach; lanes 7, kidney; lanes 8, skeletal muscle; lanes 9, heart; lanes 10, brain. The arrowheads indicate the position of ezrin (81 kDa) or moesin (77 kDa).

three closely related proteins consisting of ezrin, moesin and radixin.

Ezrin and moesin have 74% overall protein sequence identity and are believed to be membrane-microfilament linking proteins. This concept arose because their protein sequences contain an N-terminal domain that shares ~37% sequence identity with the corresponding region of erythrocyte band 4.1 (Gould et al., 1989; Lankes and Furthmayr, 1991), a well characterized membrane-microfilament linking protein (Anderson and Lovrien, 1984; Marchesi, 1985). Additional support for this hypothesis comes from recent immunolocalization studies, which show that both proteins are highly enriched in actin-containing surface structures in various cultured cell lines (Franck et al., 1993), and from ezrin cDNA transfection studies (Algrain et al., 1993).

The third member of the protein family, radixin, was purified from hepatic adherens junctions and is an F-actin barbed end-capping protein (Tsukita et al., 1989) that shares 75% sequence identity with ezrin and 81% with moesin (Funayama et al., 1991; Sato et al., 1992). Previous immunolocalization studies showed that radixin was concentrated in adherens junctions, focal contacts and the cleavage furrow (Sato et al., 1991; Tsukita et al., 1989). However, the interpretation of these results is not clear because the radixin antibodies also recognize ezrin and moesin (Sato et al., 1992). Recent results obtained using antibodies specific for ezrin or moesin revealed that these proteins are concentrated in actin-rich surface structures but not adherens junctions or focal contacts (Franck et al., 1993). Therefore, radixin must be a component of the two latter structures.

Our goal in this study was to determine the cellular distributions of ezrin and moesin with respect to F-actin in tissue sections to gain insight into the proposed function of these two highly related cytoskeletal proteins. The results indicate that ezrin and moesin serve related but distinct functions in the assembly or maintenance of actin-containing surface structures in vivo.

MATERIALS AND METHODS

Materials

Human placenta was obtained from consenting patients at Tompkins Community Hospital (Ithaca, NY). Adult female CD-1 (32-40 g) or Balb/c (25-32 g) mice, and Sprague-Dawley rats were purchased from Charles River Laboratories (Wilmington, MA). All animals had free access to food and water.

Rabbit antisera to human ezrin, human moesin and chicken villin were prepared and purified on immobilized antigen as described (Bretscher and Weber, 1979; Bretscher, 1989; Franck et al., 1993). Affinity-purified antibodies against human moesin were adsorbed against purified human ezrin to eliminate detectable cross-reactivity with the latter protein (Franck et al., 1993). Other immunoreagents were purchased from the following suppliers: rabbit antiserum against human von Willebrand factor (IgG fraction; Sigma Chemical Co., St. Louis, MO), peroxidase-conjugated goat anti-rabbit IgG (IgG fraction; Cappel, Durham, NC), fluorescein-labeled goat anti-rabbit IgG (affinity-purified; ICN, Irvine, CA), goat anti-rabbit IgG-10 nm gold (BioCell; Ted Pella, Inc., Redding, CA), normal goat serum (Gibco Laboratories, Grand Island, NY).

Immunoblot analysis

Tissues were homogenized in double-strength Laemmli sample buffer (Laemmli, 1970) and boiled for 2 min. Extracts were clarified by centrifugation, and total proteins (~25 μg) were subjected to electrophoresis in 10% SDS-polyacrylamide gels (Laemmli, 1970). Proteins were transferred to nitrocellulose with a semi-dry electroblotter (Integrated Separation Systems, Hyde Park, MA). Blots were blocked in a buffer (TBS: 50 mM Tris-HCl, 150 mM NaCl, pH 7.4) containing 3% bovine serum albumin and 0.1% Tween-20, followed by incubation with a primary antibody (30 ng/ml anti-ezrin; 50 ng/ml anti-moesin) diluted in the same buffer. After several washes, blots were treated with 2 μg/ml peroxidase-conjugated goat anti-rabbit IgG and then washed again. Finally, bound antibodies were visualized by enhanced chemiluminescence (Amersham, Arlington Heights, IL).

Immunofluorescence microscopy

Tissues were rinsed with saline, immersed briefly in OCT embedding compound (Tissue-Tek; Miles Laboratories, Inc., Naperville, IL), transferred to aluminum foil molds containing OCT, and then frozen in liquid nitrogen. Embedded specimens were stored at −70°C. Frozen sections, 6-10 μm thick, were cut on a cryostat, mounted on gelatin-coated glass microscope slides, and dried at room temperature. Sections were fixed for 30 min in 2% formaldehyde in PBS, pH 7.4, rinsed with PBS, and then treated with absolute ethanol for 5 min at −20°C to permeabilize cells. After rinsing with TBS, free aldehydes were quenched by treatment for 1 h with 150 mM glycine in TBS. Sections were blocked for 30 min in TBS containing 5% normal goat serum (TBSNGS), and then were incubated for 1 h at 37°C in a primary antibody diluted in TBSNGS (5 μg/ml anti-ezrin, 15 μg/ml anti-moesin, 25 μg/ml anti-villin, or 1:500 anti-von Willebrand factor), or buffer alone. After rinsing with TBS, sections were stained for 1 h at 37°C with

a mixture of 5 μg/ml fluorescein-labeled goat anti-rabbit IgG and a 1:50 dilution of rhodamine-labeled phalloidin (Molecular Probes, Inc., Eugene, OR), both in TBSNGS. Next, sections were washed extensively with TBS and then mounted in TBS containing 50% glycerol and 1% *n*-propyl gallate (Giloh and Sedat, 1982).

Specimens were viewed with a Zeiss Universal fluorescence microscope and images were recorded on Kodak T-Max 400 film (Eastman Kodak Co., Rochester, NY).

Immunogold cytochemistry

Tissues were rinsed briefly with saline, minced in fixative (0.1% glutaraldehyde, 4% formaldehyde, 0.2% picric acid, 0.5 mM $CaCl_2$ and 2 mM $MgCl_2$ in 0.1 M phosphate buffer, pH 7.4), and then fixed for an additional 2-3 h at room temperature. Tissues were post-fixed with uranyl acetate, dehydrated in acetone, and embedded in LR Gold resin (Polysciences, Warrington, PA) as described previously (Berryman and Rodewald, 1990).

Immunogold staining of plastic thin sections was performed at room temperature (Berryman and Rodewald, 1990). The primary antibody concentration was 3 μg/ml for ezrin and the secondary 10 nm colloidal gold-labeled goat anti-rabbit IgG was diluted 1:100. Sections were examined at 60 kV in a Philips 301 electron microscope (Philips Electronic Instruments Inc., Mahawah, NJ).

RESULTS

Tissue distribution of ezrin and moesin

The relative abundance of ezrin and moesin was examined in different mouse tissues by immunoblot analysis (Fig. 1) using specific antibodies that distinguish between the two proteins (Franck et al., 1993). Antibody concentrations were adjusted to give similar signals for equivalent amounts of the human proteins. Since equal amounts of total proteins were loaded on each lane, the relative abundance of ezrin and moesin could be estimated. Ezrin was present at high levels in intestine, stomach, lung and kidney, and to a lesser extent in spleen. In addition to p81 ezrin, some of the tissues contained an additional ~55 kDa band, which is probably a degradation product, since the first major proteolytic digestion product of ezrin is this size (Franck et al., 1993). Moreover, prolonged incubation (2 h) of kidney in ice-cold saline enhanced the 55 kDa species with concomitant loss of the p81 immunoreactive species (not shown). Moesin was most abundant in lung and spleen, and was detected at lower levels in kidney. In contrast to ezrin, moesin appeared to be more resistant to degradation; a similar finding has been reported for the purified proteins in vitro (Franck et al., 1993).

Cellular distribution of ezrin and moesin: general comments

We studied the distribution of ezrin and moesin relative to F-actin by double-label fluorescence microscopy in cryostat sections from a variety of tissues. In some cases, villin was used as an additional immunocytochemical marker. Immunoelectron microscopy was used to analyze the subcellular distribution of ezrin in cells that gave particularly intense fluorescence staining. The moesin-specific antibody proved unsuitable for immunoelectron microscopy. Since only selected examples of tissues enriched in these proteins could be presented, a summary of the results, including

Table 1. Summary of the cellular distributions of ezrin and moesin in various tissues

Organ and cell type	Ezrin	Moesin
Placenta		
Syncytiotrophoblast	+++*	±
Endothelium	−	++
Tongue		
Stratified epithelium	++	−
Endothelium	−	++
Striated muscle	−	−
Esophagus		
Stratified epithelium	++	−
Endothelium	−	++
Smooth muscle	−	−
Stomach		
Surface mucous	++*	−
Parietal	+++*	−
Chief	++*	−
Endothelium	−	++
Smooth muscle	−	−
Visceral mesothelium	+++*	−
Small intestine		
Absorptive epithelium†	+++*	−
Lymphocyte	+	+
Endothelium	−	+
Smooth muscle	−	−
Visceral mesothelium	+++*	−
Large intestine		ND§
Surface epithelium†	++*	
Gland epithelium†	−	
Smooth muscle	−	
Visceral mesothelium	+++*	
Salivary gland		ND§
Intercalated duct	++*	
Interlobular duct	+++*	
Pancreas		
Intercalated duct	++*	+*
Interlobular duct	+++*	−
Endocrine cell	−	−
Endothelium	−	++
Liver		
Hepatocyte	−	++*
Sinusoid	−	+
Large bile duct	+++*	−
Visceral mesothelium	+++*	−
Heart		
Cardiac muscle (myocardium)	−	−
Endothelium (endocardium)	−	++
Mesothelium (epicardium)	+++*	−
Lung		
Terminal bronchiole	+++*	−
Alveolar tissue	±‡	+++‡
Pleural mesothelium	+++*	−
Spleen		
Lymphocyte	+	+
Endothelium	−	++
Visceral mesothelium	+++*	−
Kidney		
Renal corpuscle	++*	+++‡
Proximal tubule†	+++*	+++*
Distal tubule	+*	±
Collecting duct	+*	±
Endothelium	−	++
Urinary bladder		
Transitional epithelium	++	−
Endothelium	−	+
Smooth muscle	−	−
Peritoneal mesothelium	+++*	−

+ and − denote relative staining intensities as judged visually by immunofluorescence microscopy. However, we cannot exclude the possibility that trace amounts of these proteins were undetected in some cells judged negative.

*Indicates a polarized distribution as determined by colocalization of ezrin or moesin with actin on the apical cell surface. The apical localization of ezrin was confirmed by immunoelectron microscopy in epithelial cells of placenta, stomach, small intestine, pancreas, kidney and mesothelia.

†Cell types in which villin was localized to the apical cell surface.

‡Cases where fluorescence staining was seen, but the identity of the cell types was not resolved with certainty. In lung, some of the moesin staining may derive from alveolar epithelial cells as well as capillary endothelia (Fig. 14e): the relatively small number of cells stained for ezrin may represent pulmonary macrophages (Fig. 9e). In the renal corpuscle, moesin may be present in podocytes as well as adjacent endothelia (Fig. 14g).

§ND, not determined.

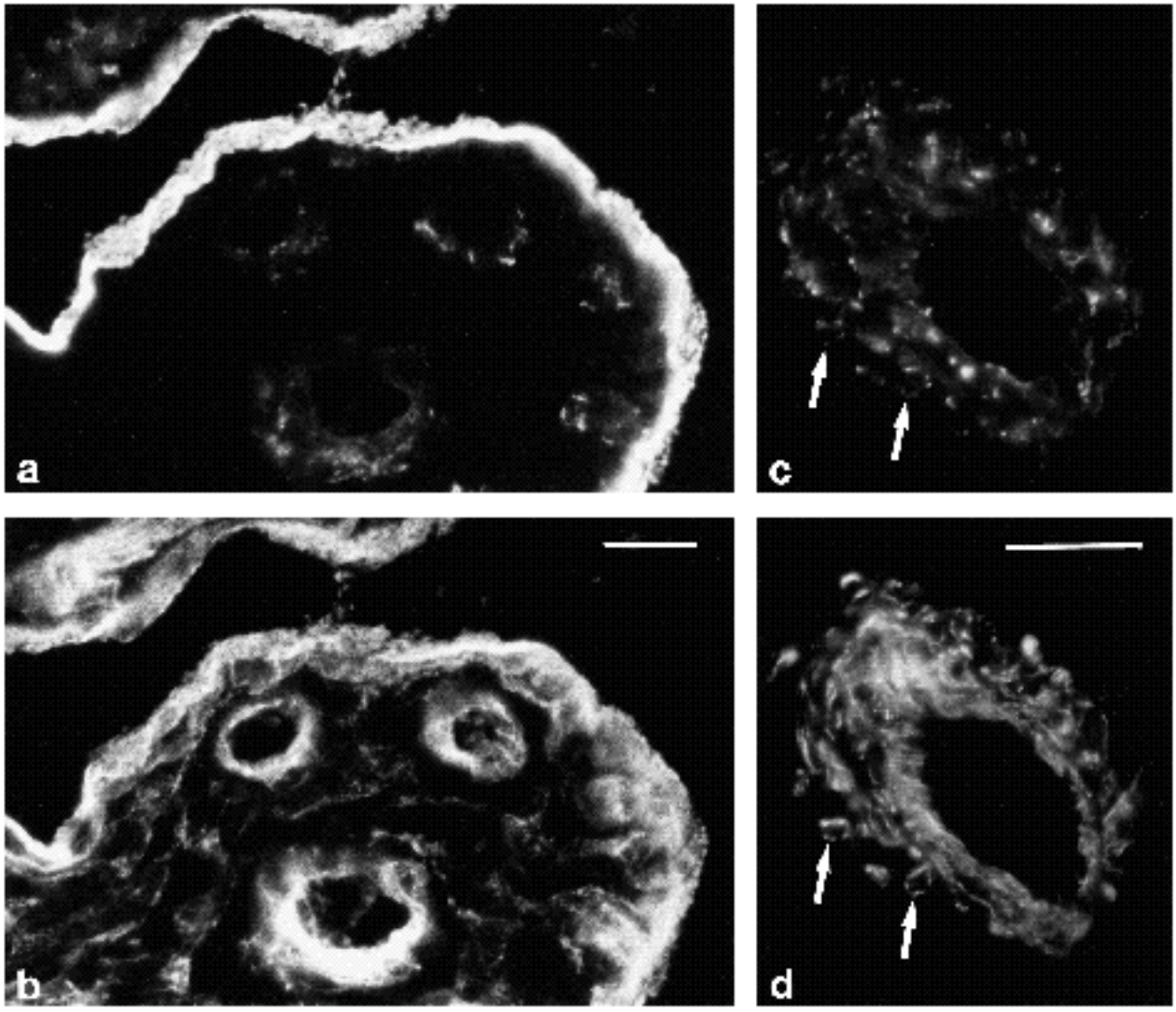

Fig. 2. Localization of ezrin (a,c) and actin (b,d) in human placenta by fluorescence microscopy. Intense staining of both ezrin (a) and actin (b) is found in trophoblasts of the chorionic villi. Ezrin is also detected in actin-rich cells located near blood vessels of the stroma (a,b). In some of these perivascular cells, a clear colocalization between ezrin and actin is seen (arrows in c,d). Bars, 20 μm.

tissues not documented photographically, is given in Table 1. The results show that ezrin and moesin are enriched in a wide variety of nonmuscle cells and are not detectable in skeletal, smooth or cardiac muscle. Because they exhibit distinct cellular distributions, their localizations are treated separately in the following sections.

Ezrin is concentrated beneath the plasma membrane in apical microvilli and other actin-containing surface structures: placenta and small intestine

Our initial studies focused on the localization of ezrin in the human placenta because we routinely use this tissue to obtain purified ezrin (Bretscher, 1989). In immunofluorescence studies, intense ezrin and actin staining was associated with syncytiotrophoblasts covering the chorionic villi (Fig. 2a,b). Immunogold staining experiments demonstrated that ezrin was highly concentrated in the apical microvilli of syncytiotrophoblasts (Fig. 3a). Gold particles appeared to be distributed randomly over the microvilli, and many particles were in close apposition to the microvillar plasma membrane. In contrast, gold particles were only rarely found on non-microvillar regions of the apical plasma membrane, including planar domains (arrows in Fig. 3b) and coated pits. Gold labeling was also sparse in the cytoplasm and on the basal plasma membrane (Fig. 3b). Cytotrophoblasts exhibited a distribution of gold labeling that was nearly identical to that on their syncytial counterparts (Fig. 4). Thus, the cytotrophoblast establishes a high degree of polarity before fusing with the syncytium.

Ezrin was also detected in some cells of the stroma of the chorionic villi (Fig. 2a,c). These cells were stained intensely for actin and appeared to be arranged concentrically around the stromal blood vessels. In some cells a clear colocalization of ezrin and actin was seen (arrows in Fig. 2c,d). Immunoelectron microscopy revealed that ezrin was enriched in cellular processes located near endothelial cells (Fig. 5). In many processes, gold particles were concen-

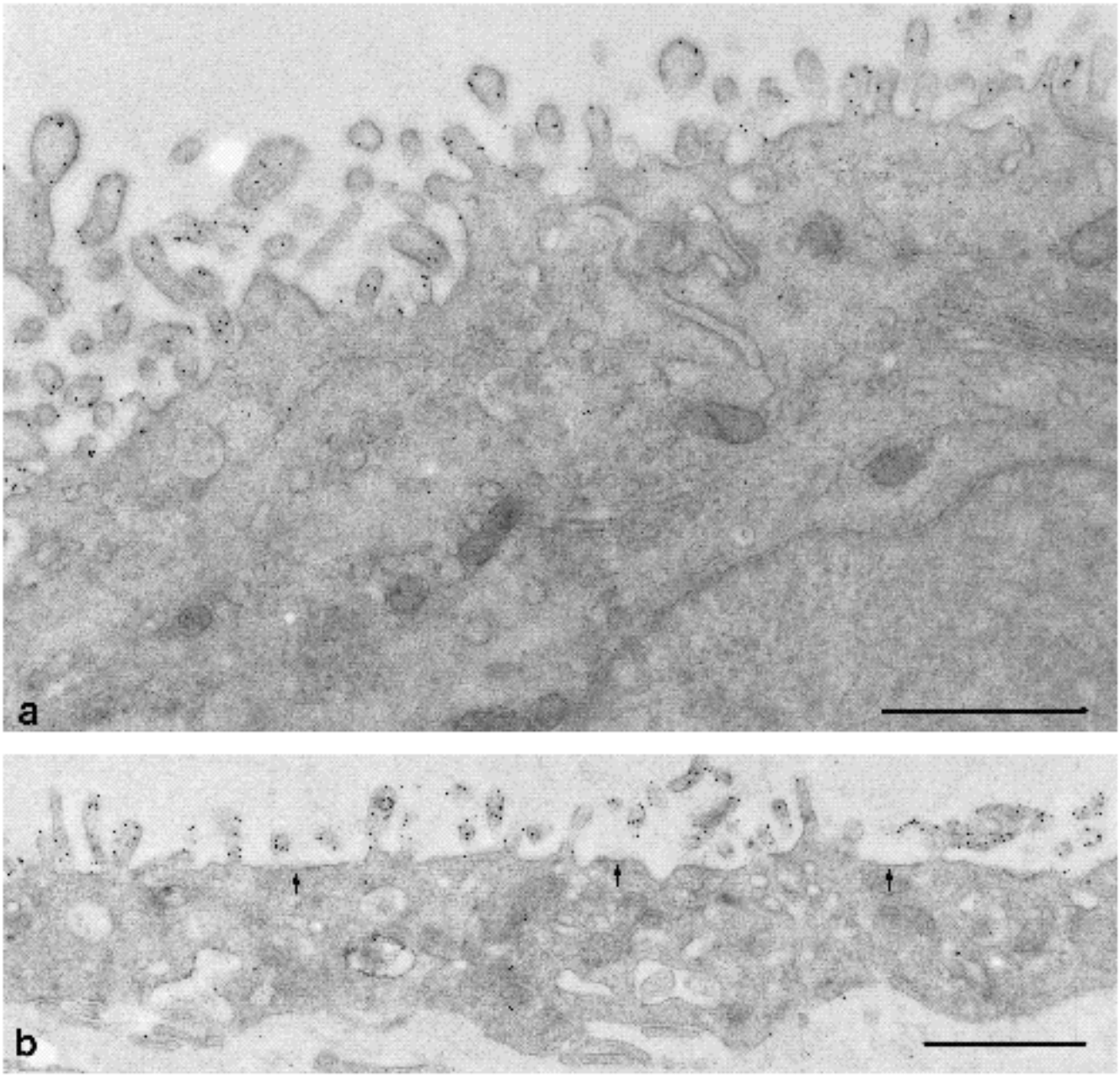

Fig. 3. Immunogold localization of ezrin in placental syncytiotrophoblasts. Gold particles are concentrated over the apical microvilli where many particles are found in close association with the plasma membrane (a). A relatively low level of gold staining is seen on planar aspects of the apical plasma membrane (arrows) and on the basal plasma membrane (b). Bars, 1 μm.

trated beneath the plasma membrane (Fig. 5b and arrows in Fig. 5a). Because we rarely observed connections between the ezrin-rich cell processes and the corresponding cell body, it was difficult to deduce the cell type.

The cellular distribution of ezrin was next examined in the small intestine because ezrin was originally isolated as a component of the intestinal microvillus cytoskeleton (Bretscher, 1983). Intense ezrin fluorescence was seen in the brush border of mature absorptive cells lining the villus (Fig. 6a). In immunogold labeling experiments, gold particles were highly concentrated over apical microvilli and appeared to be distributed randomly along their length (Fig. 7a). In longitudinal and tangential sections, it was difficult to determine whether the gold particles were associated preferentially with the plasma membrane or the microvillus cores. As described by Drenckhahn and Dermietzel (1988), the interpretation of the staining patterns in these orientations is complicated by at least three factors: (1) the inherent curvature of the microvilli; (2) the diameter of the microvilli is similar to the thickness of the section (~0.1 μm); and (3) the gold particles only stain antigens at the surface and do not penetrate into the section. However, in transverse sections of brush border microvilli these problems were minimal, and most gold particles were localized on or near the plasma membrane (Fig. 7b).

In regions where the mature brush border was cut tan-

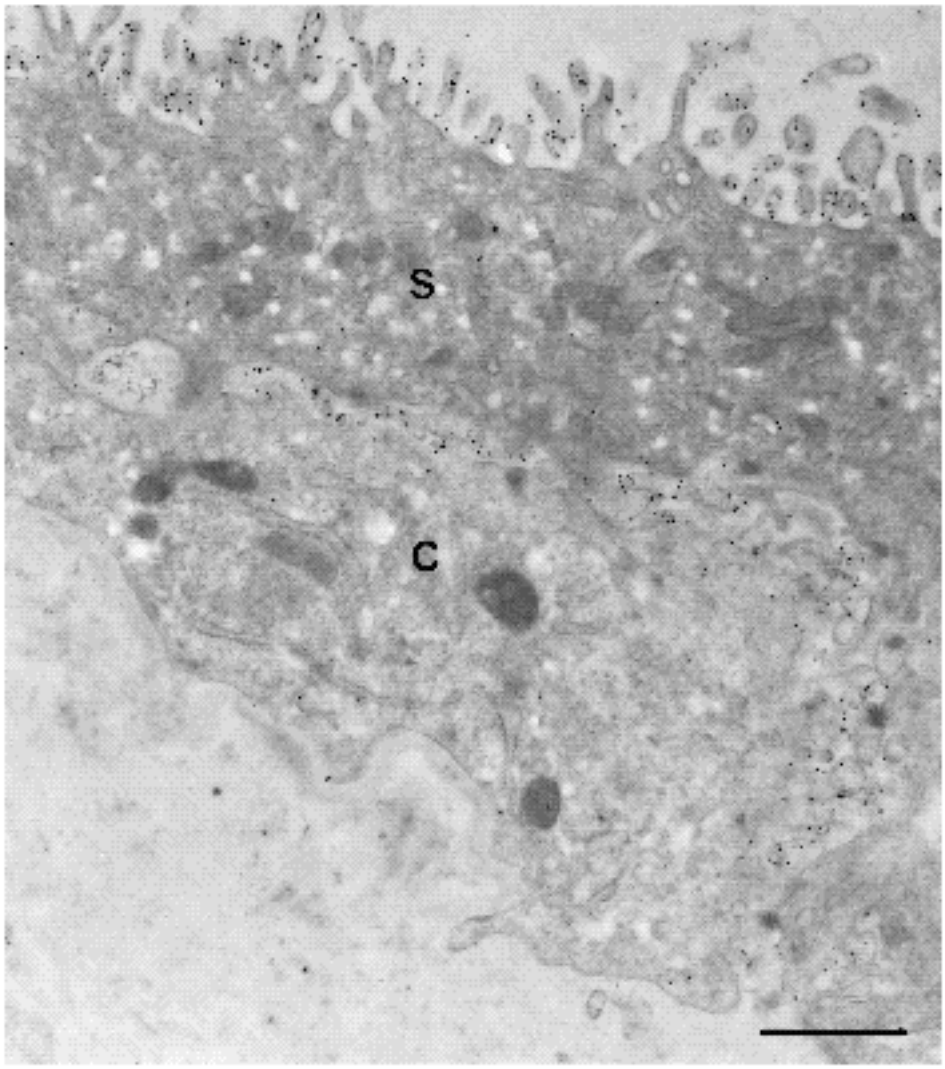

Fig. 4. Polarized distribution of ezrin in a cytotrophoblast. Gold staining is concentrated over the apical surface of the cytotrophoblast (C), specifically over the loosely organized microvillar-like structures adjacent to the basal surface of the overlying syncytium (S). As with syncytial cells (see Fig. 3b), only a few gold particles are found on the basal plasma membrane of the cytotrophoblast. Bar, 1 μm.

gentially, a honeycomb pattern of intense actin staining was seen, presumably representing cell-cell adherens junctions (Fig. 6b, inset). In contrast, ezrin staining was diffuse in these regions and showed no evidence of the pattern that characterizes these junctions (Fig. 6a, inset). By immunoelectron microscopy, gold particles were rarely associated with the adherens junctions (Fig. 7a, bracket).

In contrast to mature cells, a low level of ezrin fluorescence was observed on the basolateral surface of immature cells in the crypts (Fig. 6a,c). The apical surface of these cells was stained intensely, but to a lesser extent than in the brush border of mature cells. In sections stained with antibodies to villin, the distribution of fluorescence in epithelial cells along the crypt-villus axis was virtually identical to what was seen for ezrin (Fig. 6, compare c and e).

Ezrin is enriched in specific classes of epithelial cells throughout the gastrointestinal tract: stomach and large intestine

We found that ezrin was enriched in several additional epithelial cell types that line the gastrointestinal tract. In the stomach, fluorescence staining of ezrin was intense and colocalized with actin in parietal cells (Fig. 8a,b). This observation is consistent with previous immunolocalization studies on isolated rabbit gastric glands (Hanzel et al., 1991). Two additional cell types in the stomach were enriched in ezrin: surface mucous cells and chief cells. In mucous (Fig. 8a,b) and chief (Fig. 8c,d) cells, ezrin colocalized with actin on the apical surface. This distribution of ezrin was confirmed by immunoelectron microscopy. Gold labeling on the apical surface was associated specifically with microvillar membranes of parietal cells, surface mucous cells and chief cells (not shown).

Fluorescence microscopy of large intestine showed that ezrin was present in the brush border of surface absorptive cells that faced the gut lumen (Fig. 8e). However, little or no ezrin was detected in cells of the intestinal glands. In contrast to ezrin, villin staining was present in the apical region of cells located on the surface and in the glands (Fig. 8f,g).

Ezrin is concentrated on the apical surface of many other simple epithelia, including duct cells of pancreas and liver, kidney proximal and distal tubules, and all mesothelia

We found that ezrin was concentrated on the apical surface

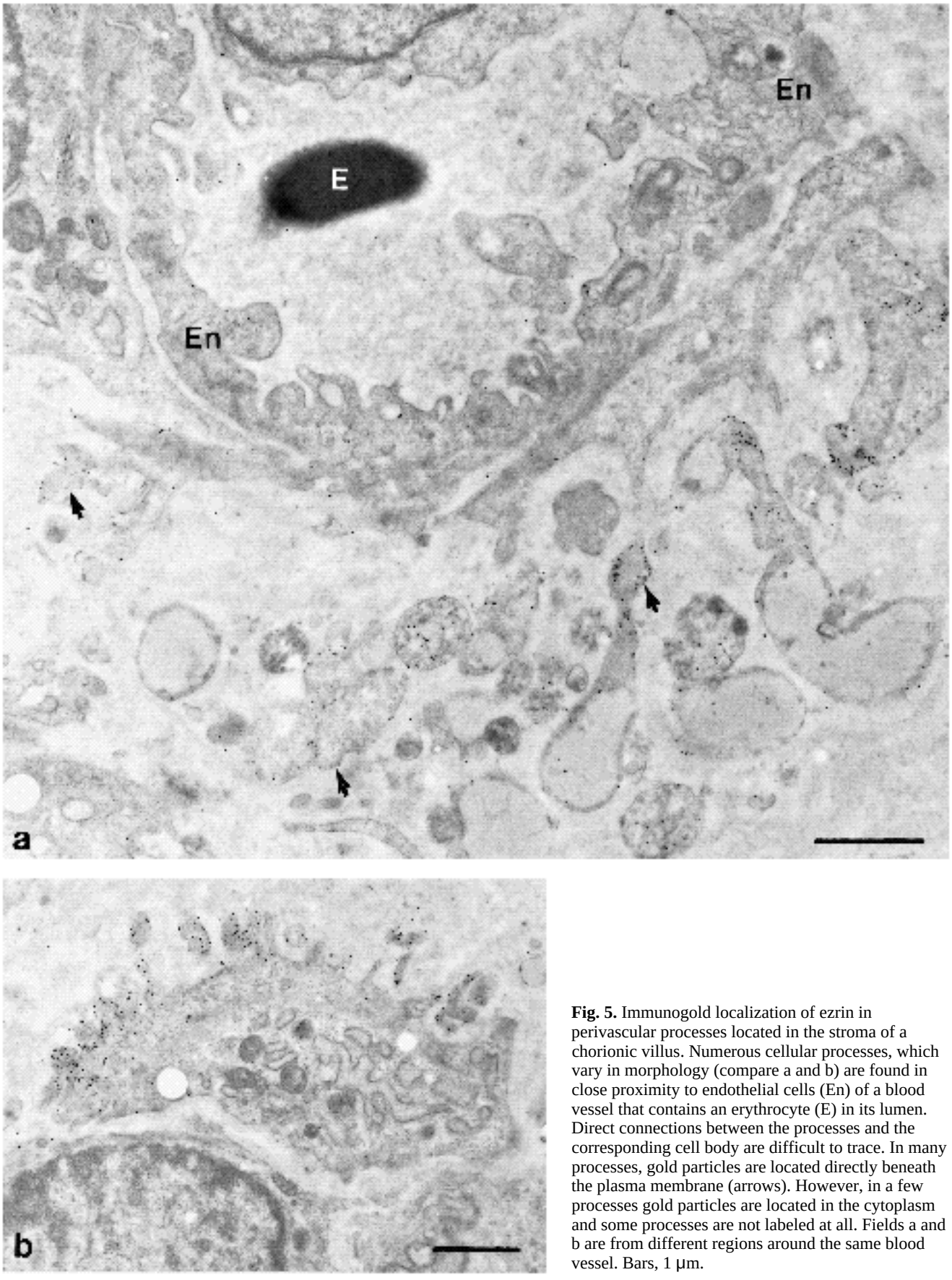

Fig. 5. Immunogold localization of ezrin in perivascular processes located in the stroma of a chorionic villus. Numerous cellular processes, which vary in morphology (compare a and b) are found in close proximity to endothelial cells (En) of a blood vessel that contains an erythrocyte (E) in its lumen. Direct connections between the processes and the corresponding cell body are difficult to trace. In many processes, gold particles are located directly beneath the plasma membrane (arrows). However, in a few processes gold particles are located in the cytoplasm and some processes are not labeled at all. Fields a and b are from different regions around the same blood vessel. Bars, 1 μm.

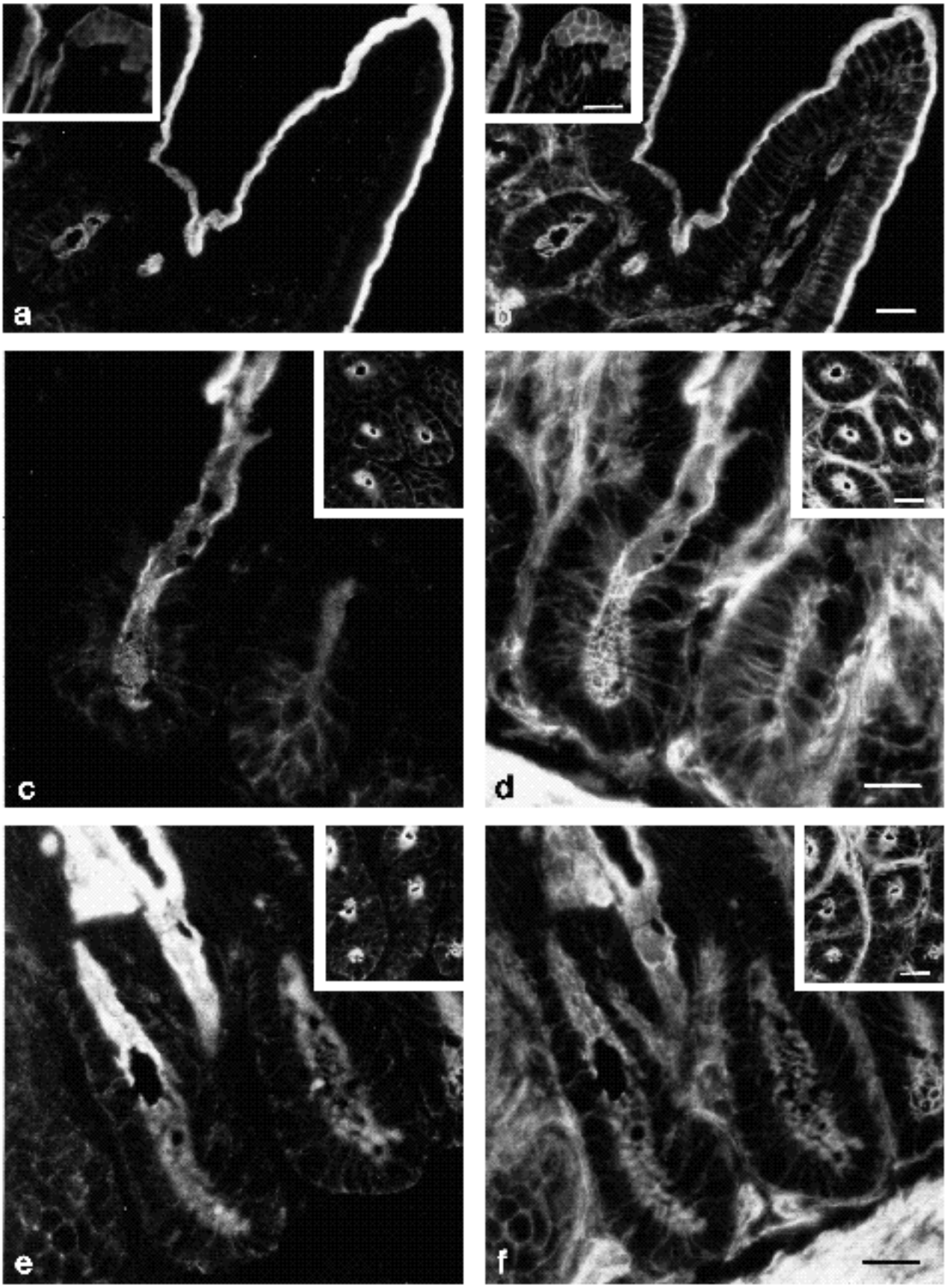

Fig. 6

of a wide variety of polarized epithelial cell types (Table 1). In the pancreas, we observed a striking colocalization between ezrin and actin on the apical surface of cells that line the intercalated ducts and larger interlobular ducts (Fig. 9a,b). A similar colocalization pattern was seen in the salivary gland (not shown). In the liver, only cells of the large bile ducts were stained with the ezrin antibody (Fig. 9c,d). Hepatocyte adherens junctions, which are rich in radixin (Tsukita et al., 1989), were seen as pairs of bright dots by actin staining (arrowheads in Fig. 9d) but were not stained for ezrin. In the lung, bright ezrin staining colocalized with actin on the apical surface of epithelial cells of the terminal bronchioles (Fig. 9e,f). We also observed occasional cells, probably macrophages, distributed throughout the alveolar tissue, that were stained for ezrin.

Because the apical surface of cells of the proximal but not distal tubule is known to be rich in villin (Bretscher et al., 1981; Robine et al., 1985), we stained adjacent tissue sections with antibodies to ezrin and villin, and found that both proteins were expressed in proximal cells (Fig. 10a,b). Cells of the distal tubules and collecting ducts exhibited a lower level of ezrin staining. Immunoelectron microscopy confirmed this cellular distribution of ezrin, and also revealed its specific localization to apical microvilli in each of these cell types (not shown). The fluorescence staining associated with the renal corpuscle demonstrated that ezrin is enriched in yet another cell type (Fig. 10a). The identity of this cell type was resolved by immunogold staining. Labeling was associated with the apical surface of podocytes, where gold particles were localized specifically to the plasma membrane of the actin-rich foot processes (not shown).

A high level of ezrin staining was detected in squamous mesothelial cells covering organs of the pleural, visceral and peritoneal cavities (Table 1). Although ezrin staining was always very intense, a relatively low level of actin staining was observed in these cells (Fig. 11a-h). Immunogold electron microscopy revealed the precise distribution of ezrin in mesothelial cells (Fig. 11i). Gold particles were concentrated exclusively over long slender microvilli, which faced the body cavity. Little or no staining was associated with non-microvillar regions of the apical plasma

Fig. 6. Fluorescence microscopy localization of ezrin (a,c), villin (e), and actin (b,d,f) in epithelial cells of mouse small intestine. Mature epithelial cells that line the villi exhibit intense staining for both ezrin and actin on the brush border surface (a,b). In tangential sections through the brush border, bright actin staining at the cell periphery forms a honeycomb pattern, which presumably depicts the cell-cell adherens junctions (b, inset). However, in these same regions ezrin staining is diffuse and does not appear to be enriched in the adherens junctions (a, inset). In contrast to mature cells, ezrin staining is found on both the apical and basolateral surfaces of immature cells located deep in the crypts seen in transverse section (insets in c,d). A longitudinal section through the crypt-villus axis shows an increase in the intensity of ezrin and actin staining on the brush border as cells exit the crypts, and that the loss of basolateral ezrin staining is abrupt (c,d). The distribution of villin along the crypt-villus axis is similar to that for ezrin (compare e and c). Neither ezrin (c) nor villin (e) is detected in smooth muscle cells, which exhibit strong actin staining (lower corners in d,f). Bars, 20 μm.

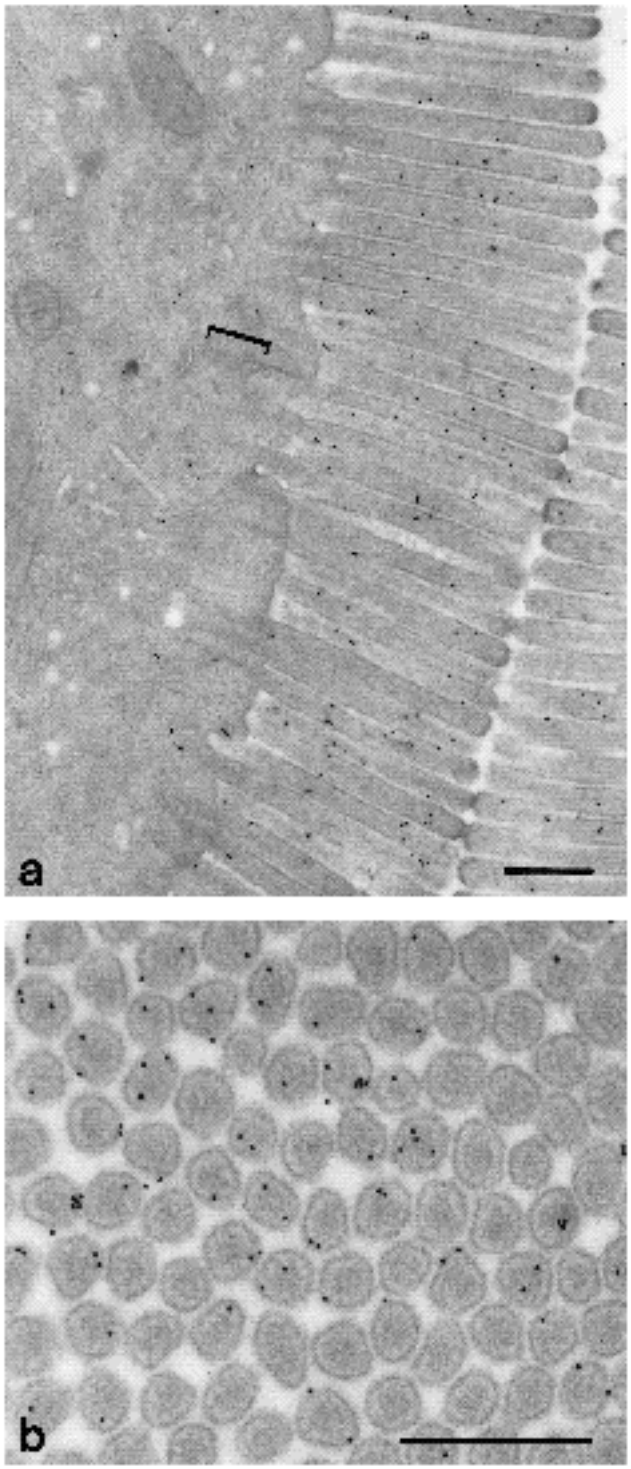

Fig. 7. Immunogold localization of ezrin in the apical region of mature epithelial cells of rat small intestine. Most gold particles are associated with the microvilli; however, a low level of staining is also seen in the terminal web region (a). No staining is seen in the region of the adherens junction (bracket). A transverse section through the microvilli shows that many gold particles are in close proximity to the plasma membrane (b). Bars, 0.5 μm.

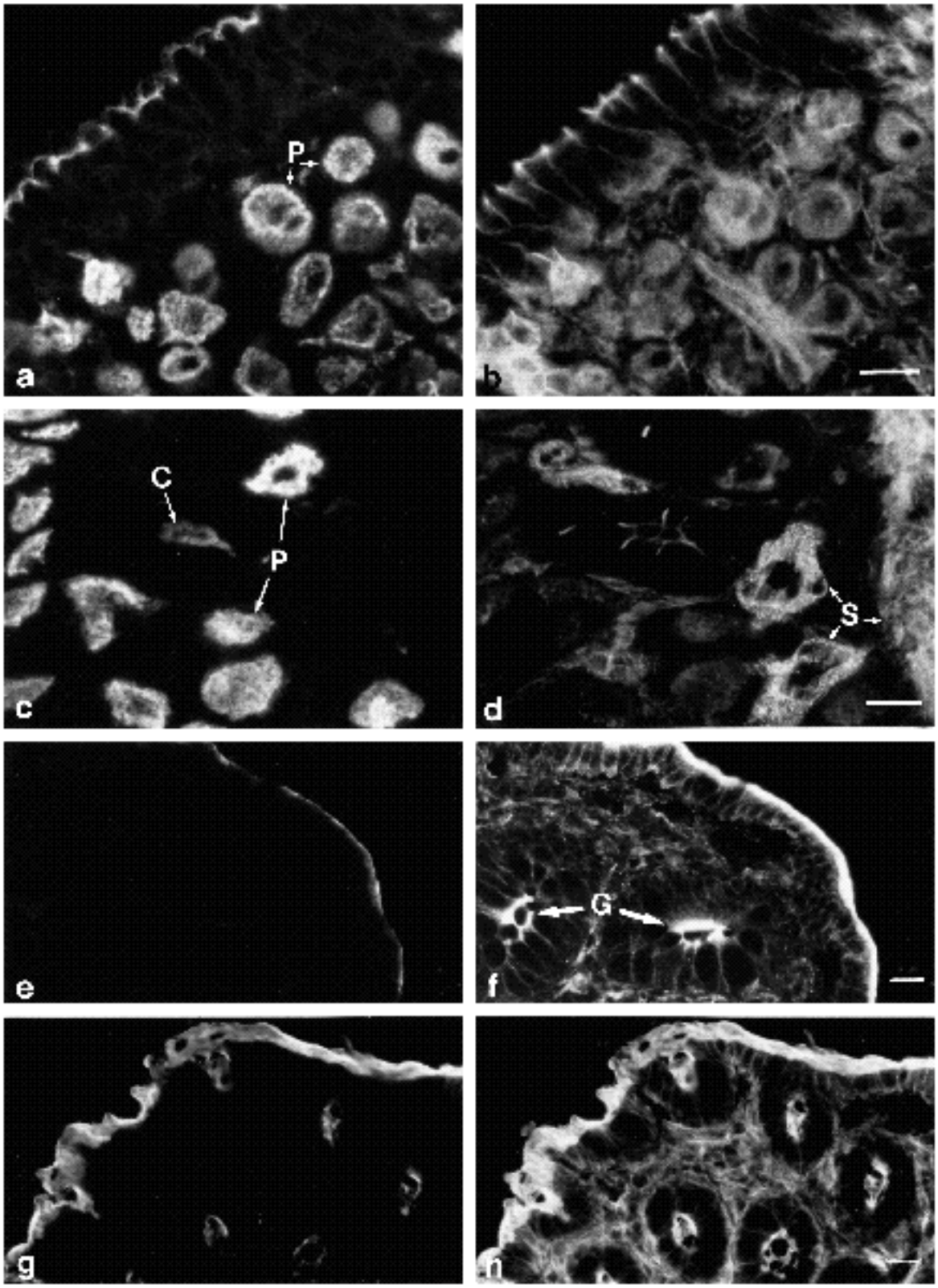

Fig. 8. Fluorescence localization of ezrin (a,c,e), villin (g) and actin (b,d,f,h) in epithelial cells of mouse stomach (a-d) and large intestine (e-h). In stomach, ezrin colocalizes with actin in gastric parietal cells (P), and on the apical surface of mucous cells facing the lumen (a,b). Ezrin also colocalizes with actin on the apical surface of chief cells (C) located deep in a gastric gland (c,d). No ezrin is detected in smooth muscle cells (vascular and muscularis smooth muscle (S) identified in d). In large intestine, ezrin staining colocalizes with actin on the brush border of surface absorptive cells but not cells located in the glands (G) (e,f). In contrast to ezrin, villin is enriched on the brush border of both surface absorptive and glandular epithelial cells (g,h). Bars, 20 μm.

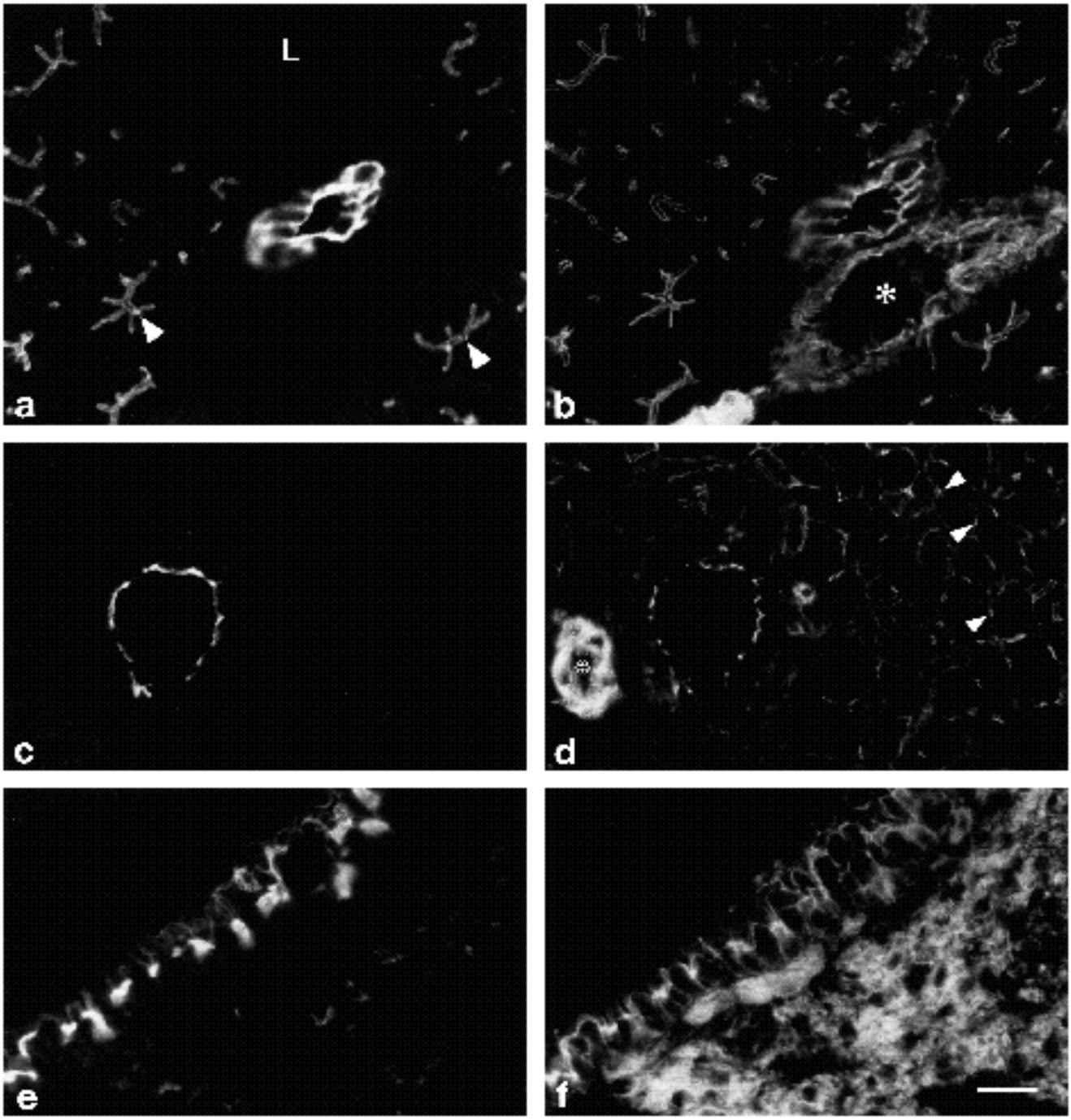

Fig. 9. Distribution of ezrin (a,c,e) and actin (b,d,f) in mouse pancreas (a,b), liver (c,d), and lung (e,f). In pancreas, ezrin and actin are colocalized on the apical surface of cells lining the intercalated ducts (arrowheads in a,b). The larger exocrine duct shows intense apical ezrin staining. No staining is detected in endocrine cells of the islet of Langerhans (L) or in blood vessels (*,b). In liver, ezrin is colocalized with actin in cells that line the large bile duct (c,d). In contrast, none is detected in hepatocytes, sinusoids or smooth muscle cells of an artery (*,d). The absence of ezrin staining in cell-cell adherens junctions (arrowheads in d) indicates that the ezrin antibody does not cross-react with radixin, which is enriched at this site (Tsukita et al., 1989). In lung, intense ezrin staining colocalizes with actin on the apical surface of epithelial cells that line the terminal bronchiole (e,f). A small subset of cells located in the underlying alveolar tissue, probably macrophages, exhibit a low level of ezrin staining. Bar, 20 μm.

ciated with non-microvillar regions of the apical plasma membrane, the cytoplasm, or the basolateral membrane.

Ezrin is also present in stratified epithelia

In addition to a broad range of simple epithelial cell types, we found that ezrin was also expressed in stratified and transitional epithelia. In tongue and esophagus, mature cells of the outermost stratified layers displayed a distribution of ezrin that was largely coincident with actin (Fig. 12a-d). The squamous phenotype of these cells was readily appar-

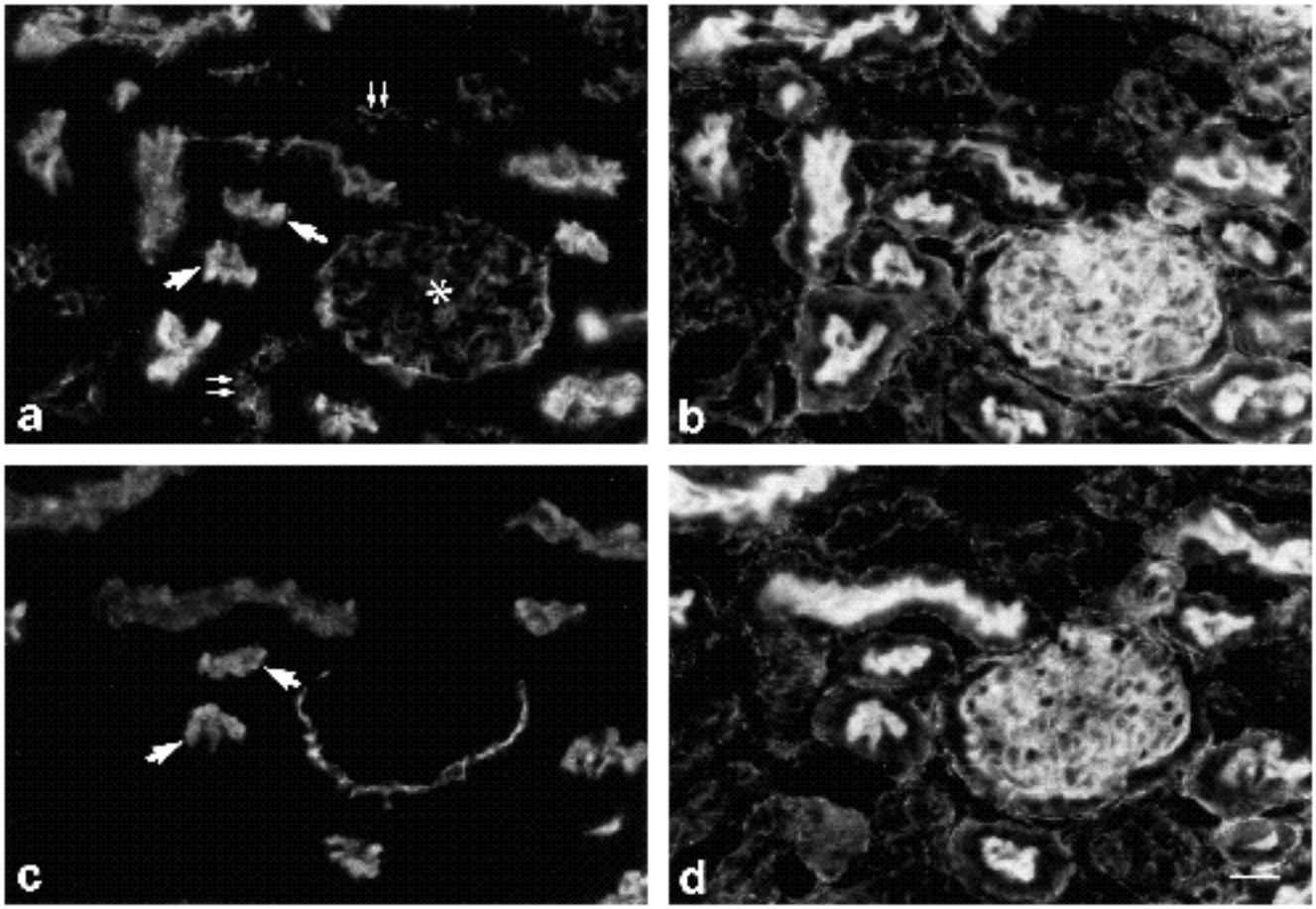

Fig. 10. Fluorescence localization of ezrin (a), villin (c) and actin (b,d) in adjacent sections of mouse kidney cortex. Ezrin and villin are colocalized with actin on the brush border of proximal tubule cells (single arrows in a,c). Ezrin staining is also associated with cells of the distal tubules (double arrows in a) and renal corpuscle (*). In contrast, no villin is detected at these sites. Bar, 20 μm.

ent because the staining was localized near the cell periphery. Immature cells near the base of the epithelium exhibited a more diffuse ezrin staining and a lower level of actin compared with mature cells. A close inspection of the epidermal stem cells revealed a somewhat polarized distribution of ezrin (arrows in Fig. 12a,c). Thus, the redistribution of ezrin correlated well with the appearance of actin at the periphery of differentiating and mature squamous cells. Ezrin was also found in transitional cells of the urinary bladder (Fig. 12e).

Moesin is enriched in endothelial cells

In all tissues examined, the staining pattern of moesin was very different from the pattern of ezrin (Table 1). Moesin was found to be enriched in endothelial cells of all tissues studied; some selected examples are shown in Fig. 13. In the stomach, the serpentine course of capillaries between adjacent gastric glands was reflected by the observed staining pattern for moesin (Fig. 13a). No staining was detected in parietal, mucous or chief cells. In the intestine moesin could not be detected in epithelial cells, but was found in lymphocytes as shown in a section through a lymph nodule (Fig. 13c,d). The endothelial location of moesin was particularly evident in splenic arteries (Fig. 13e). In longitudinal and transverse sections, moesin was clearly confined to the center of these vessels when compared with the distribution of actin in the surrounding smooth muscle (Fig. 13e,f). Although it was difficult to document the colocalization of moesin with actin in endothelial cells, this can be seen in the transverse section of the splenic artery shown in the insets (Fig. 13e,f). The localization of moesin to endothelial cells was also clearly evident in the heart (Fig. 13g,h). No moesin staining was detected in cardiac intercalated discs, structures that are known to be rich in radixin (Tsukita et al., 1989). We confirmed the endothelial location of moesin by immunofluorescence studies in which adjacent tissue sections (placenta and tongue) were stained with antibodies to von Willebrand factor (Jaffe et al., 1973) and moesin, revealing a precise colocalization between these two antigens in capillaries and larger blood vessels (not shown). Moesin was not detected in stratified epithelial cells, epithelial cells of the gastrointestinal tract (Fig. 13a,c), or mesothelial cells.

Moesin is also present in certain epithelial cell types

Moesin was colocalized with actin on the apical surface of a very restricted set of polarized epithelial cell types. In the pancreas, moesin was readily detected in capillary endothelial cells, especially in the islets of Langerhans (Fig.

14a). A low but detectable level of moesin staining colocalized with actin on the apical surface of intercalated ducts (arrows in Fig. 14a,b), which also contained ezrin (Fig. 9a). However, in contrast to ezrin, larger interlobular ducts were not stained with the moesin antibody (double arrows in Fig. 14a,b). The cellular distributions of moesin and ezrin were mutually exclusive in the liver and the lung. A moderate level of moesin staining colocalized with actin on the apical surface of hepatocytes (Fig. 14c; compare with ezrin in Fig. 9c), but none was detected in cells of the large bile ducts. Intense moesin fluorescence was seen in alveolar tissue of the lung, but no staining was detected in epithelial cells of the terminal bronchiole (Fig. 14e; compare with ezrin in Fig. 9e). Because of the fragile nature of lung tissue and the limited resolution of the light microscope, we were unable to determine whether this high level of moesin staining was due to its presence in squamous epithelial cells, endothelial cells or both. Surprisingly, the brush border of the kidney proximal tubule was found to contain high levels of moesin (Fig. 14g,h) in addition to actin, villin and ezrin (Fig. 10a-d). Intense moesin staining was also localized to the renal corpuscle (Fig. 14g). However, we were unable to resolve whether this staining was restricted to endothelial cells or was contributed by podocytes as well.

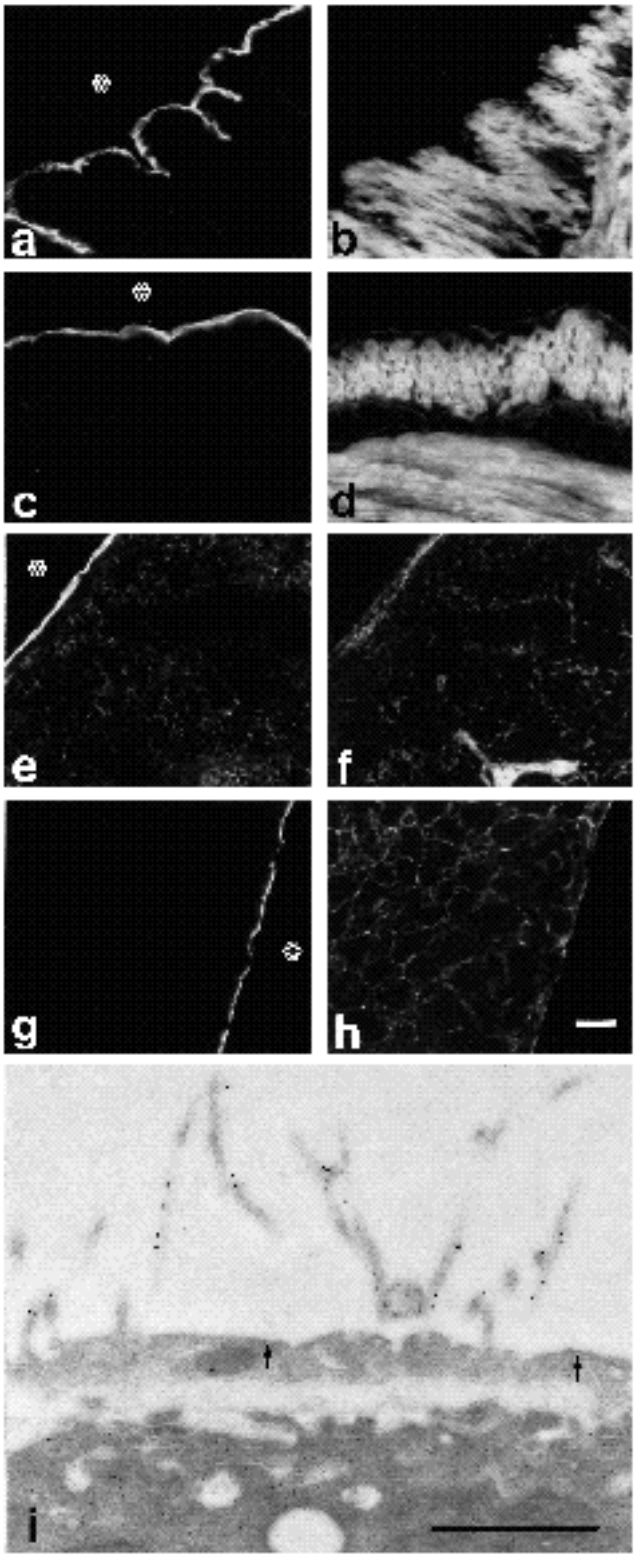

DISCUSSION

The aim of this study was to determine the distributions of the two closely related proteins, ezrin and moesin. Because of the ~75% sequence identity between ezrin, moesin and radixin, it is important to address the issue of antibody specificity. Sato et al. (1992) described several antibodies that reacted with all three members of the protein family, ezrin, moesin and radixin. However, recent results from our laboratory indicate that the antibodies used in the current study are specific for either ezrin or moesin (Franck et al., 1993). We show here that ezrin and moesin have very different cellular distributions, confirming that our antibodies distinguish between these two proteins. A number of observations indicate that these antibodies do not detect radixin. Ezrin and moesin were not enriched in intestinal or hepatic adherens junctions, or cardiac intercalated discs, locations that are known to be rich in radixin (Tsukita et al., 1989). Moreover, neither of our antibodies stain focal contacts of cultured cells (Franck et al., 1993), structures stained by antibodies that recognize all three members of the ezrin, moesin and radixin protein family (Sato et al., 1992). Thus, we conclude that our antibody preparations are specific for either ezrin or moesin.

Fig. 11. Localization of ezrin in mesothelia. Cryosections of stomach (a,b), large intestine (c,d), spleen (e,f) and liver (g,h) were labeled for ezrin (a,c,e,g) and actin (b,d,f,h). Intense ezrin staining is seen in mesothelial cells adjacent to the body cavity (*). Ezrin is not detected in smooth muscle cells of the stomach (a) or large intestine (c). A relatively low level of actin staining is seen in the mesothelium compared with the intensely stained smooth muscle (b,d). Beneath the mesothelium in spleen, a large number of cells, many of which are lymphocytes, exhibit staining for both ezrin (e) and actin (f). In liver, ezrin staining is localized exclusively to mesothelial cells and is not detected in the underlying hepatic tissue (g,h). Immunogold localization of ezrin in mouse liver mesothelium (i). Gold particles are distributed specifically over long, slender microvilli that project into the body cavity. No gold labeling is seen on planar aspects of the apical plasma membrane between the sparsely distributed microvilli (arrows) or on the basal membrane. The underlying hepatocyte is not stained. Bars: (a-h) 20 μm; (i) 1 μm.

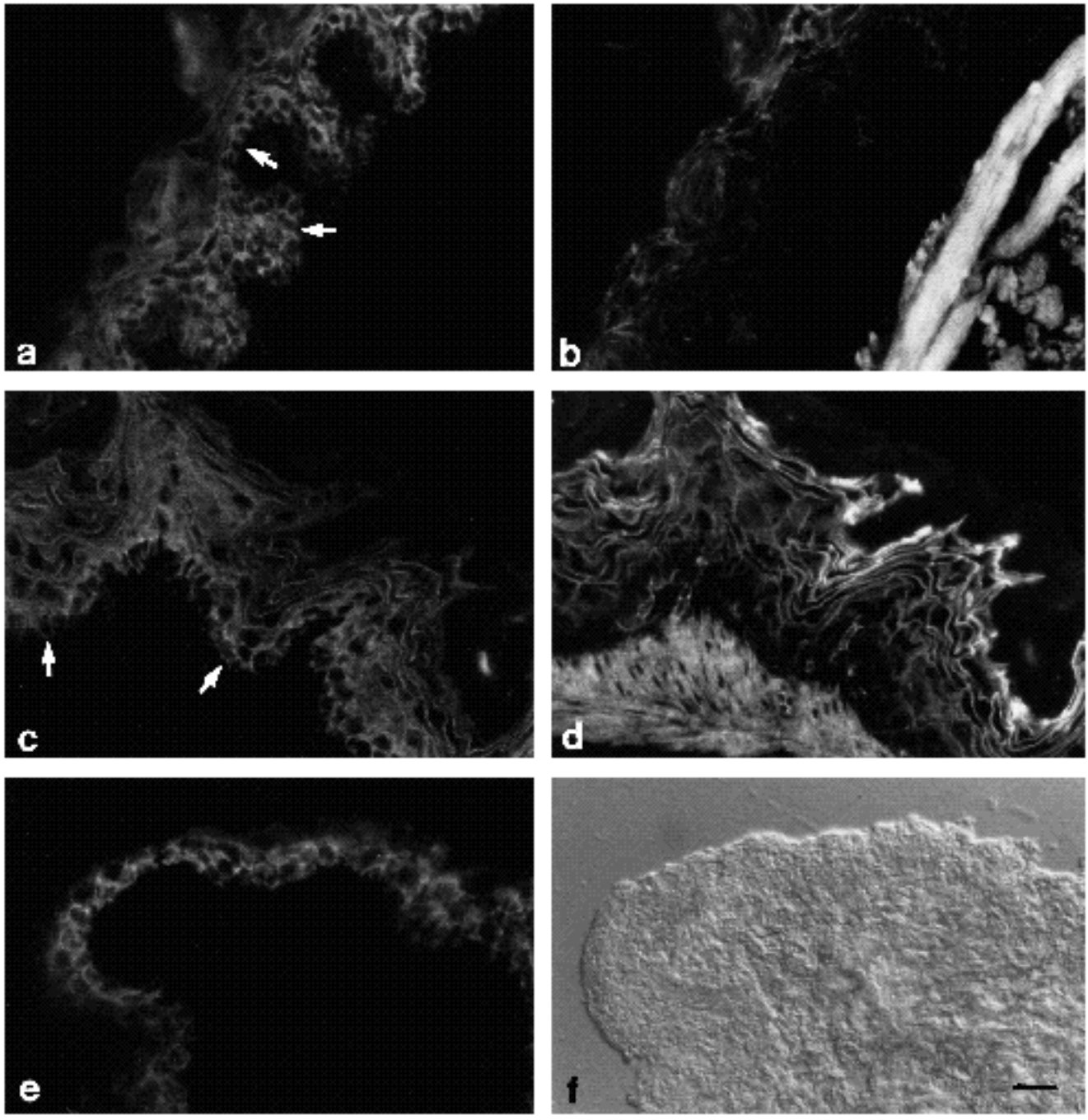

Fig. 12. Localization of ezrin (a,c,e) and actin (b,d) in stratified (a-d) and transitional epithelia (e). In tongue (a,b) and esophagus (c,d), squamous cells of the outer strata show a peripheral staining pattern for both ezrin and actin (a-d). Cuboidal cells of the basal strata exhibit a somewhat polarized and diffuse ezrin staining (arrows in a,c). A low level of actin staining is seen in these cells compared with more differentiated squamous cells. No ezrin is detected in cells of the lamina propria, striated muscle cells or smooth muscle cells. Transitional cells of urinary bladder exhibit ezrin staining but none is seen in the underlying lamina propria (e). The corresponding Nomarski image is shown in (f). Bar, 20 μm.

Fig. 13. Distribution of moesin (a,c,e,g) and actin (b,d,f,h) in mouse stomach (a,b), small intestine (c,d), spleen (e,f) and heart (g,h). In stomach, moesin staining is seen in capillaries located between the gastric glands (a) but little or no specific staining is detected in parietal cells, or in mucous cells that face the lumen (upper right corner in a and b) (compare with ezrin in Fig. 8a). In intestine, a low level of moesin staining is detected in lymphocytes of a lymphoid nodule (L), but none is seen in the overlying absorptive epithelial cells (c,d) (compare with ezrin in Fig. 7c). In spleen, moesin staining is enriched in endothelial cells of arteries cut longitudinally (arrows in e) and transversely (inset). Note that the actin-rich vascular smooth muscle cells (f) are not stained for moesin. In heart, moesin staining is localized to capillary endothelial cells (arrows in g) interspersed among the cardiac muscle fibers, which show no specific staining. A vein (V) that was cut tangentially exhibits moesin staining on its luminal aspect but none is seen in the surrounding smooth muscle. Bar, 20 μm.

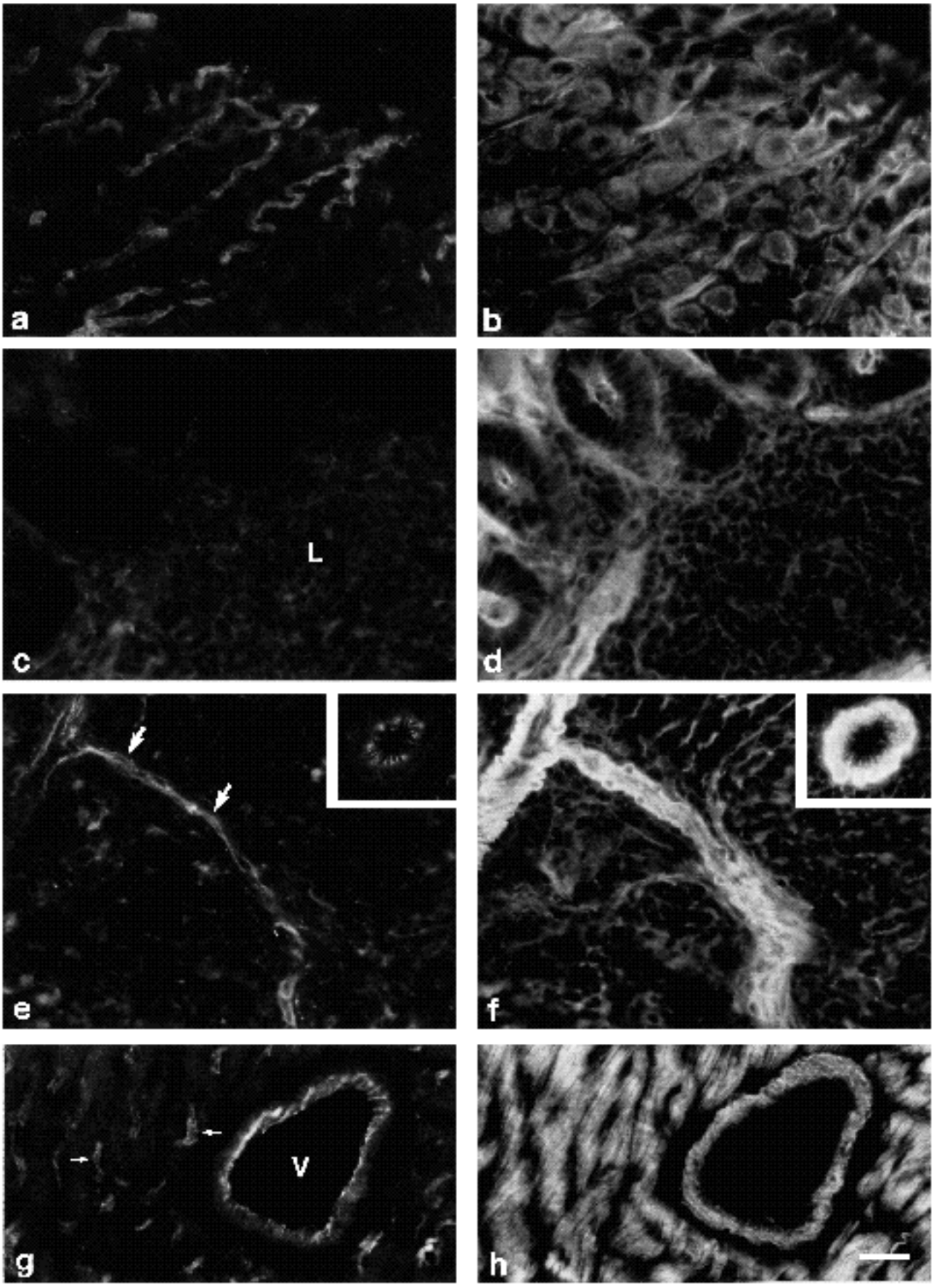

Fig. 13

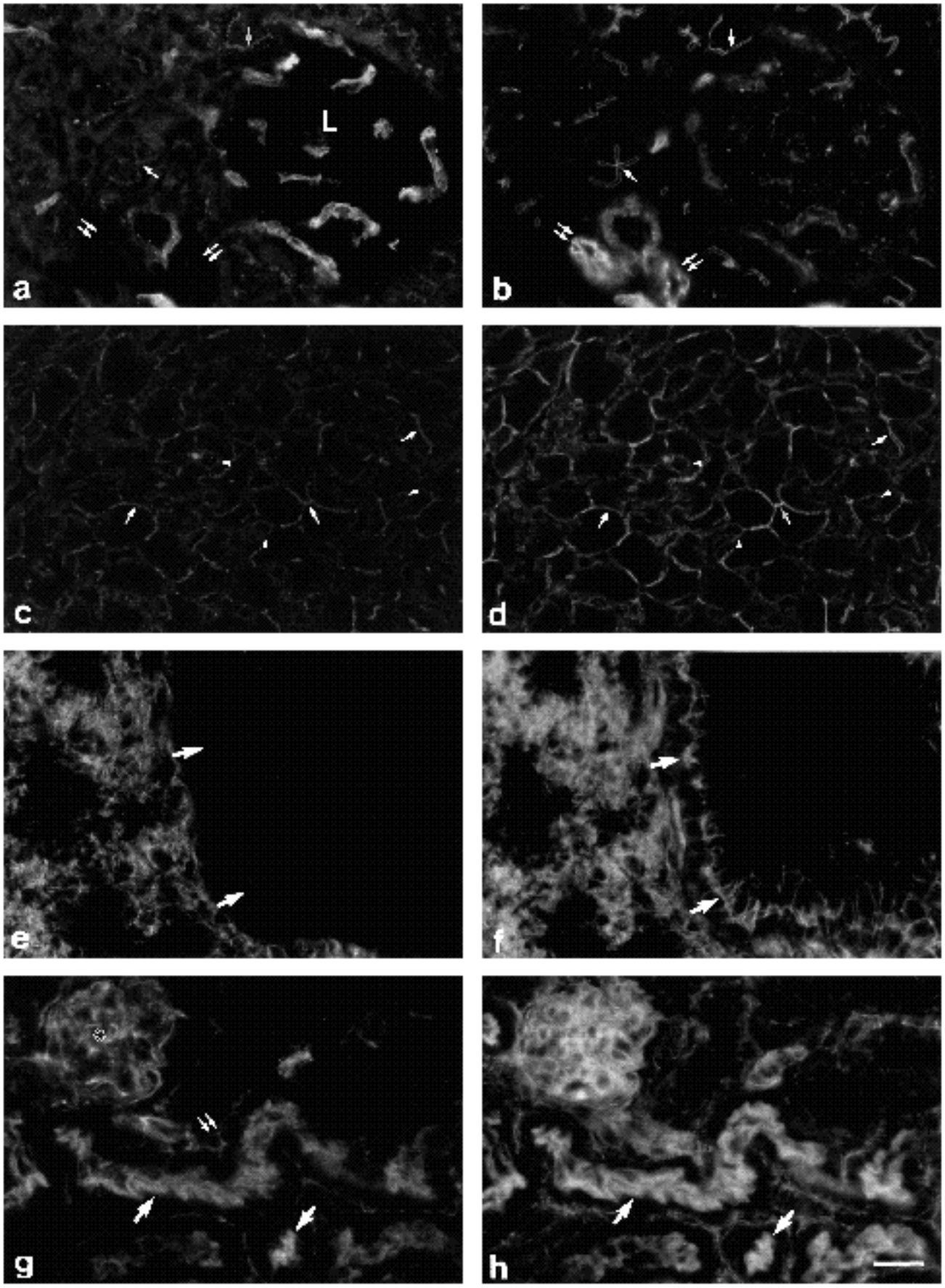

Fig. 14

Ezrin in microvilli and other actin-containing surface structures

Our results demonstrate that ezrin is highly enriched and colocalizes with actin at the apical surface of many types of simple epithelial cells that have microvilli. Thus, in these cells ezrin serves as an excellent marker for surface polarity. The clearest examples of this polarized distribution include epithelial cells of the small intestine, syncytiotrophoblasts of the placenta, mesothelia, and cells of the kidney proximal tubule. By immunoelectron microscopy, the vast majority of ezrin on the apical surface was restricted specifically to microvillar domains of the plasma membrane (Figs 3b,11i). In contrast, domains of the plasma membrane between microvilli including planar regions and coated pits, and other membrane invaginations were essentially free of ezrin. This highly restricted localization is unique among known cytoskeletal proteins. Because the distribution of ezrin along the length of the microvilli appeared random, it seems unlikely that ezrin is an F-actin barbed-end capping protein like radixin (Tsukita et al., 1989), but rather a direct or indirect F-actin side-binding protein.

Even in cases where the polarized distribution of ezrin was not evident by light microscopy, we found a striking polarized distribution of ezrin by immunoelectron microscopy. For example, in placenta we have found that filopodia or ruffles, probably from pericytes or leukocytes, were specifically and highly enriched in ezrin (Fig. 5). In addition, ezrin was found on the plasma membrane of the actin-rich foot processes of glomerular podocytes. These localizations in microvilli and other surface structures that contain actin implicate ezrin as a peripheral membrane protein, probably as a membrane-cytoskeletal linker, involved in the assembly or maintenance of these structures.

The suggestion that ezrin might play a role in the assembly or stabilization of actin-containing cell surface structures (Bretscher, 1989; Hanzel et al., 1991) is consistent with our current findings on the distribution of ezrin in differentiating intestinal epithelial cells. These cells are derived from a population of undifferentiated stem cells that proliferate continually within the crypt, followed by programmed differentiation and migration out of the crypt and along the length of the villus. During differentiation, selected cytoskeletal proteins accumulate at the apical pole of the cell in an orderly fashion and assemble a mature brush border (Bretscher, 1991; Louvard et al., 1992). Villin is the first major actin-binding protein known to become restricted to the apical domain during brush border assembly, suggesting that it may be important for the initial phases of the process. Our results show that ezrin increases in abundance and concentrates at the apical surface of differentiating enterocytes in a manner similar to villin, placing both proteins in a location consistent with an assembly function. Additional evidence to support this view comes from studies in cells lacking villin, which show that ezrin becomes highly enriched in the microvilli and membrane ruffles induced by treatment of cultured A-431 cells with epidermal growth factor (Bretscher, 1989). Together, these observations indicate that ezrin may be required for the proper formation and assembly of microvilli in the intestine and, by extrapolation, in other systems.

Fig. 14. Fluorescence microscopy localization of moesin (a,c,e,g) and actin (b,d,f,h) in endothelial cells and epithelial cells of mouse pancreas (a,b), liver (c,d), lung (e,f) and kidney (g,h). In pancreas, intense moesin staining is localized to capillary endothelial cells; this localization is readily apparent in the islet of Langerhans (L) because the endocrine cells are not stained. Moesin appears to be marginally enriched at the apical surface of the intercalated ducts (arrows in a,b), but little or none is detected in larger exocrine ducts (double arrows in a,b) (compare with ezrin in Fig. 9a). In liver, moesin is enriched and colocalizes with actin in the bile canaliculi, which correspond to the apical surface of hepatocytes (arrows in c,d). A barely detectable level of fluorescence is seen in the sinusoids (arrowheads) (compare with ezrin in Fig. 9c). In lung, intense moesin staining is found in the alveolar tissue (e), which exhibits intense actin staining (f). However, no moesin is detected in epithelial cells that line the terminal bronchiole (arrows in e,f) (compare with ezrin in Fig. 9e). In kidney, intense moesin staining colocalizes with actin on the brush border of proximal tubule cells (arrows in g,h) and in cells of the renal corpuscle (*) (compare with ezrin in Fig. 10a). Staining is also seen in endothelial cells situated between adjacent tubules (double arrows, g). Bar, 20 μm.

Cellular distribution of ezrin and moesin

To date, the functions of these proteins are unknown, so we anticipated that a detailed study of their localizations in the variety of cell types in the body would provide insight into their physiological roles. Because ezrin and moesin are coexpressed in many cultured cell lines (Franck et al., 1993; Sato et al., 1992) and colocalize with actin in surface microvilli and membrane ruffles (Franck et al., 1993), we expected that the two proteins would be distributed similarly in vivo. To our surprise, we found that ezrin and moesin have almost mutually exclusive cellular distributions, although some clear and interesting exceptions to this rule are evident (Table 1). Particularly clear examples of this distinction include stratified epithelial cells, epithelial cells of the gastrointestinal tract, cells of the terminal bronchiole, and mesothelia, all of which expressed ezrin but lacked detectable moesin. Conversely, endothelial cells and hepatocytes expressed moesin but lacked detectable ezrin. It is interesting to note that mesothelial and endothelial cells are both squamous epithelial cells of mesenchymal origin, yet in their differentiated state express only ezrin or moesin, respectively.

A theme that emerges from this study is that the expression of ezrin and moesin is regulated in a cell-type specific fashion in vivo. So why are ezrin and moesin both expressed in most cultured cell lines, including epithelial cells and fibroblasts (Franck et al., 1993; Sato et al., 1992), yet in vivo many epithelial cells do not appear to contain moesin, and connective tissue fibroblasts lacked detectable levels of both proteins? Why is ezrin readily detected in cultured hepatocytes (Franck et al., 1993), yet not detected in liver tissue? We suggest that when cells are adapted to grow in culture they frequently begin to express ezrin and/or moesin, perhaps in response to changes in growth factors or extracellular matrix components. We have begun to test this adaptation hypothesis. In preliminary experiments, primary cultures of human umbilical vein endo-

thelial cells initially expressed only moesin, whereas after 8-10 passages both proteins were detected. Perhaps such adaptation can explain why Lankes et al. (1988) found that smooth muscle cells express moesin in culture, yet in this study we found that smooth muscle cells lack moesin in vivo. Although the cell type-specific expression of ezrin and moesin in cultured cells does not always reflect what is seen in tissues, their localizations to microvilli in cultured cells are nevertheless consistent with their observed localizations to microvilli in vivo.

A major finding is that the microvilli of nearly all polarized epithelial cell types are selectively enriched in either ezrin or moesin, or sometimes both proteins (Table 1). Although ezrin was found in virtually all microvilli, one exception was the apical microvilli of hepatocytes, which contained moesin but not ezrin. Some microvilli appear to be enriched in both ezrin and moesin. A particularly clear case is the brush border microvilli that line the kidney proximal tubules. Because kidney and intestinal brush border microvilli both contain actin, villin, fimbrin, myosin I (Bretscher and Weber, 1979, 1980; Bretscher et al., 1981; Coluccio, 1991; Rodman et al., 1986) and ezrin, the presence of moesin in kidney but not intestinal microvilli is the first known biochemical difference in their cytoskeletal compositions and may relate to their different ultrastructures. In addition to polarized epithelia, ezrin and moesin were both found in lymphocytes, a cell type that is known to contain abundant microvilli. This coexpression and alternative expression of ezrin and moesin in surface microvilli suggests a related but distinct function for the two proteins. Moreover, the presence of moesin and absence of detectable ezrin in endothelial cells supports this notion. Recent studies in cultured cells have shown that antibodies that cross-react with ezrin, moesin and radixin stain adherens junctions and focal contacts (Sato et al., 1992) but not antibodies specific for either ezrin or moesin (Franck et al., 1993). Therefore, since only radixin is concentrated in cell-cell adherens junctions and focal contacts, it appears that this closely related protein has a function that is different from ezrin or moesin.

Our data support the hypothesis that ezrin and moesin are membrane-cytoskeletal linking proteins (Algrain et al., 1993; Gould et al., 1989; Lankes and Furthmayr, 1991). The differential expression of these proteins suggests that they have distinct linking properties that are adapted to particular cell types. For example, a membrane protein that is common among various types of polarized epithelial cells may associate with the cytoskeleton via ezrin whereas a different membrane protein that is common to endothelia and certain polarized epithelia may associate with the cytoskeleton via moesin. Alternatively, ezrin or moesin may bind to a variety of different membrane proteins, each of which is expressed in a cell type-specific manner. This latter possibility is supported by evidence from other systems. For example, in gastric parietal cells ezrin probably binds to the proton pump in the apical microvilli (Hanzel et al., 1991). Since this proton pump is cell type-specific, ezrin must bind to a different membrane protein in other cells. Ankyrin provides a precedent for such alternate binding partners: in erythrocytes it binds band 3 whereas in epithelial cells it binds the β-subunit of the Na^+/K^+-ATPase (Morrow et al., 1989; Nelson and Veshnock, 1987). Thus, we suggest that ezrin may be important for establishing or maintaining surface polarity in functionally diverse types of epithelial cells, by tethering specific apical membrane proteins to the actin cytoskeleton. Likewise, moesin may play a related role in endothelial and selected epithelial cells. The challenge now is to identify the other components that participate in this linkage and determine how the assembly and disassembly of these linkages are regulated.

We thank Ron Gary for critical reading of the manuscript, Matt Footer for help with fluorescence microscopy, and Janet Krizek for help with antibody preparation. Additional thanks go to the Doctors and staff at Tompkins Community Hospital for helping us obtain placental tissue and to Dr Drew Noden for the use of his cryostat. This work was funded by a grant from the National Institutes of Health (GM36652) to A. Bretscher. M. Berryman was supported by a postdoctoral fellowship from the NIH (GM14352).

This work was presented in part at the 32nd annual meeting for the American Society for Cell Biology and has appeared in abstract form (*Molecular Biology of the Cell* (1992) **3**, 364a).

REFERENCES

Algrain, M., Turunen, O., Vaheri, A., Louvard, D. and Arpin, M. (1993). Ezrin contains cytoskeleton and membrane binding domains accounting for its proposed role as a membrane-cytoskeletal linker. *J. Cell Biol.* **120**, 129-139.

Anderson, R. A. and Lovrien, R. E. (1984). Glycophorin is linked by band 4.1 protein to the human erythrocyte membrane skeleton. *Nature* **307**, 655-658.

Berryman, M. A., and Rodewald, R. D. (1990). An enhanced method for post-embedding immunocytochemical staining which preserves cell membranes. *J. Histochem. Cytochem.* **38**, 159-170.

Birgbauer, E. and Solomon, F. (1989). A marginal band-associated protein has properties of both microtubule- and microfilament-associated proteins. *J. Cell Biol.* **109**, 1609-1620.

Bretscher, A. (1983). Purification of an 80,000-dalton protein that is a component of the isolated microvillus cytoskeleton, and its localization in nonmuscle cells. *J. Cell Biol.* **97**, 425-432.

Bretscher, A. (1989). Rapid phosphorylation and reorganization of ezrin and spectrin accompany morphological changes induced in A-431 cells by epidermal growth factor. *J. Cell Biol.* **108**, 921-930.

Bretscher, A. (1991). Microfilament structure and function in the cortical cytoskeleton. *Annu. Rev. Cell Biol.* **7**, 337-374.

Bretscher, A., Osborn, M., Wehland, J. and Weber, K. (1981). Villin associates with specific microfilamentous structures as seen by immunofluorescence microscopy on tissue sections and cells microinjected with villin. *Exp. Cell Res.* **135**, 213-219.

Bretscher, A. and Weber, K. (1979). Villin: the major microfilament-associated protein of the intestinal microvillus. *Proc. Nat. Acad. Sci. USA* **76**, 2321-2325.

Bretscher, A. and Weber, K. (1980). Fimbrin: a new microfilament-associated protein present in microvilli and other cell surface structures. *J. Cell Biol.* **86**, 335-340.

Coluccio, L. (1991). Identification of the microvillar 110-kDa calmodulin complex (myosin-1) in kidney. *Eur. J. Cell Biol.* **56**, 286-294.

Drenckhahn, D. and Dermietzel, R. (1988). Organization of the actin filament cytoskeleton in the intestinal brush border: a quantitative and qualitative immunoelectron microscope study. *J. Cell Biol.* **107**, 1037-1048.

Drenckhahn, D. and Mannherz, H. G. (1983). Distribution of actin and the actin-associated proteins myosin, tropomyosin, alpha actinin, vinculin and villin in rat and bovine exocrine glands. *Eur. J. Cell Biol.* **30**, 167-176.

Ezzel, R. M., Chafel, M. M. and Matsudaira, P. T. (1989). Differential localization of villin and fimbrin during development of the mouse visceral endoderm and intestinal epithelium. *Development* **106**, 407-419.

Franck, Z., Footer, M. and Bretscher, A. (1990). Microinjection of villin into cultured cells induces rapid and long-lasting changes in cell morphology but does not inhibit cytokinesis, cell motility, or membrane ruffling. *J. Cell Biol.* **111**, 2475-2485.

Franck, Z., Gary, R. and Bretscher, A. (1993). Moesin, like ezrin, colocalizes with actin in the cortical cytoskeleton in cultured cells, but its expression is more variable. *J. Cell Sci.* **105**, 219-232.

Friederich, E., Huet, C., Arpin, M. and Louvard, D. (1989). Villin induces microvilli growth and F-actin redistribution in transfected fibroblasts. *Cell* **59**, 461-475.

Friederich, E., Vancompernolle, K., Huet, C., Goethals, M., Finidori, J., Vandekerckhove, J. and Louvard, D. (1992). An actin-binding site containing a conserved motif of charged amino acid residues is essential for the morphogenic effect of villin. *Cell* **70**, 81-92.

Funayama, N., Nagafuchi, A., Sato, N., Tsukita, S. and Tsukita, S. (1991). Radixin is a novel member of the band 4.1 family. *J. Cell Biol.* **115**, 1039-1048.

Giloh, H. and Sedat, J. W. (1982). Fluorescence microscopy: reduced photobleaching of rhodamine and fluorescein protein conjugates by *n*-propyl gallate. *Science* **217**, 1252-1255.

Goslin, K., Birgbauer, E., Banker, G. and Solomon, F. (1989). The role of cytoskeleton in organizing growth cones: a microfilament-associated growth cone component depends upon microtubules for its localization. *J. Cell Biol.* **109**, 1621-1631.

Gould, K. L., Bretscher, A., Esch, F. S. and Hunter, T. (1989). cDNA cloning and sequencing of the protein-tyrosine kinase substrate, ezrin, reveals homology to band 4.1. *EMBO J.* **8**, 4133-4142.

Gould, K. L., Cooper, J. A., Bretscher, A. and Hunter, T. (1986). The protein-tyrosine kinase substrate, p81, is homologous to a chicken microvillar core protein. *J. Cell Biol.* **102**, 660-669.

Hanzel, D. K., Urushidani, T., Ursinger, W. R., Smolka, A. and Forte, J. G. (1989). Immunological localization of an 80kDa phosphoprotein to the apical membrane of gastric parietal cells. *Amer. J. Physiol.* **256**, 1082G-1089G.

Hanzel, D., Reggio, H., Bretscher, A., Forte, J. G. and Mangeat, P. (1991). The secretion-stimulated 80K phosphoprotein of parietal cell is ezrin, and has properties of a membrane cytoskeletal linker in the induced apical microvilli. *EMBO J.* **10**, 2363-2373.

Heintzelman, M. B. and Mooseker, M. S. (1990a). Structural and compositional analysis of early stages in microvillus assembly in the enterocyte of the chick embryo. *Differentiation* **43**, 175-182.

Heintzelman, M. B. and Mooseker, M. S. (1990b). Assembly of the brush border cytoskeleton: changes in the distribution of microvillar core proteins during enterocyte differentiation in adult chicken intestine. *Cell Motil. Cytoskel.* **15**, 12-22.

Jaffe, E. A., Hachman, R. I., Becker, C. G. and Minick, R. C. (1973). Culture of human endothelial cells derived from umbilical vein: identification by morphologic and immunologic criteria. *J. Clin. Invest.* **52**, 2745-2756.

Laemmli, U. K. (1970). Cleavage of structural proteins during the assembly of the head of bacteriophage T4. *Nature* **227**, 680-685.

Lankes, W. T. and Furthmayr, H. (1991). Moesin: a member of the protein 4.1-talin-ezrin family of proteins. *Proc. Nat. Acad. Sci. USA* **88**, 8297-8301.

Lankes, W., Griesmacher, A., Grunwald, J., Schwartz-Albiez, R. and Keller, R. (1988). A heparin-binding protein involved in inhibition of smooth-muscle cell proliferation. *Biochem. J.* **251**, 831-842.

Louvard, D., Kedinger, M. and Hauri, H. P. (1992). The differentiating intestinal epithelial cell: establishment and maintenance of functions through interactions between cellular structures. *Annu. Rev. Cell Biol.* **8**, 157-195.

Marchesi, V. T. (1985). Stabilizing infrastructure of cell membranes. *Annu. Rev. Cell Biol.* **1**, 531-561.

Maunoury, R., Robine, S., Pringault, E., Huet, C., Guénet, J. L., Gaillard, J. A. and Louvard, D. (1988). Villin expression in the visceral endoderm and in the gut enlarge during early mouse embryogenesis. *EMBO J.* **7**, 3321-3329.

Morrow, J. S., Cianci, D. C., Ardito, T., Mann, A. S. and Kashgarian, M. (1989). Ankyrin links fodrin to the alpha subunit of the Na, K-ATPase in Madin-Darby canine kidney cells and in intact renal tubule cells. *J. Cell Biol.* **108**, 455-465.

Nelson, W. J. and Veshnock, P. J. (1987). Ankyrin binding to (Na^+, K^+) ATPase and implications for the organization of membrane domains in polarized cells. *Nature* **328,** 533-536.

Pakkanen, R. (1988). Immunofluorescent and immunochemical evidence for the expression of cytovillin in the microvilli of a wide range of cultured human cells. *J. Cell. Biochem.* **38**, 65-75.

Pakkanen, R., Hedman, K., Turunen, O., Wahlstrom, T. and Vaheri, A. (1987). Microvillus-specific Mr 75,000 plasma membrane protein of human choriocarcinoma cells. *J. Histochem. Cytochem.* **35**, 809-816.

Pakkanen, R., von Bonsdorff, C.-H., Turunen, O., Wahlstrom, T. and Vaheri, A. (1988). Redistribution of Mr 75,000 plasma membrane protein, cytovillin, into newly formed microvilli in herpes simplex and Semliki Forest virus infected human embryonal fibroblasts. *Eur. J. Cell Biol.* **46**, 435-443.

Robine, S., Huet, C., Moll, R., Sahuquillo-Merino, C., Coudrier, E., Zweibaum, A. and Louvard, D. (1985). Can villin be used to identify malignant and undifferentiated normal digestive epithelial cells? *Proc. Nat. Acad. Sci. USA* **82**, 8488-8492.

Rodman, J. S., Mooseker, M. and Farquhar, M. G. (1986). Cytoskeletal proteins of the rat kidney proximal tubule brush border. *Eur. J. Cell Biol.* **42**, 319-327.

Sato, N., Funayama, N., Nagafuchi, A., Yonemura, S., Tsukita, S. and Tsukita, S. (1992). A gene family consisting of ezrin, radixin and moesin: its specific localization at actin filament/plasma membrane association sites. *J. Cell Sci.* **103**, 131-143.

Sato, N., Yonemura, S., Obinata, T., Tsukita, S. and Tsukita, S. (1991). Radixin, a barbed end-capping actin-modulating protein, is concentrated at the cleavage furrow during cytokinesis. *J. Cell Biol.* **113**, 321-330.

Shibayama, T., Carboni, J. M. and Mooseker, M. S. (1987). Assembly of the intestinal brush border: appearance and redistribution of microvillar core proteins in developing chick enterocytes. *J. Cell Biol.* **105**, 335-344.

Tsukita, S., Hieda, Y. and Tsukita, S. (1989). A new 82-kD barbed end-capping protein (radixin) localized in the cell-to-cell adherens junction: purification and characterization. *J. Cell Biol.* **108**, 2369-2382.

Urushidani, T., Hanzel, D. K. and Forte, J. G. (1989). Characterization of an 80-kDa phosphoprotein involved in parietal cell stimulation. *Amer. J. Physiol.* **256**, G1070-G1081.

(Received 4 February 1993 - Accepted 12 April 1993)